Electrical and Structural Properties of Thin Palladium Films

R. Anton
Institut für Angewandte Physik der Universität, Hamburg

K. Häupl *, P. Rudolf **, and P. Wißmann
Institut für Physikalische und Theoretische Chemie der Universität, Erlangen

Z. Naturforsch. **41 a**, 665–670 (1986); received January 25, 1986

The electrical resistivity of thin palladium films deposited on amorphous substrates is measured in dependence on film thickness. The data are interpreted with the help of a statistical model taking into account structural information obtained from AES, TEM and x-ray diffraction texture analysis. The steep decrease of resistivity in the ultra-thin thickness region can be immediately correlated with the formation of coherent areas in the films. A more flattened course is reached at about 8 nm thickness where a continuous film structure develops.

1. Introduction

Recently several groups have reported new results on the physical and chemical properties of thin palladium films [1, 2]. These films are of actual interest either as alloy components during the formation of MOS devices on the basis of silicon technology in microelectronics, or as catalysts for the CO oxidation. For basic research the films are deposited on amorphous substrates under UHV conditions [3–8] ensuring a clean surface without incorporated gases. The structure of such films has been investigated only sporadically [5–8]. In particular, there is a lack of information on the correlation between electrical and structural data. With the present paper we intend to provide a better understanding in this area.

2. Resistivity Measurements

Details of the experimental set-up are described elsewhere [9]. In the present case, small Pyrex glass plates served as substrates (dimensions 10 mm × 5 mm × 1 mm). The plates were fire-polished and supplied with two molybdenum contacts (evaporated layers of about 1 μ thickness). The resistance was measured in situ under ultrahigh-vacuum conditions, the thickness was monitored with the help of a vibrating quartz oscillator (Varian model 985-7010). Palladium was deposited from a specpure wire by current heating with a rate of 0.4 nm/min at ambient temperature. Suhrmann et al. described the details of the pretreatment of the palladium wire with hydrogen [3].

A typical set of experimental points is shown in Figure 1. The measured resistance R had been transformed into the resistivity ϱ by

$$\varrho = R\,d/F\,, \tag{1}$$

where d is the film thickness. The geometric factor F was determined to be $F = 1,45$ for the substrates used here.

3. AES Measurements

In order to get an insight into the structural properties we have deposited films of various thicknesses on partially oxidized Si(100) wafers in a separate pumping device which was supplied with an AES spectrometer. For details of the preparation techniques refer to Anton [10]. The substrates were annealed for 1 h at 800 °C under ultrahigh-vacuum conditions before depositing the palladium. After this annealing treatment only carbon traces smaller than 0.1% of a monolayer were detected in the AES spectrum.

The thickness dependence of the peak-to-peak intensity of some characteristic AES peaks is shown in Figure 2. The 330 eV peak of palladium (○) increases linearly with thickness in the beginning of the deposition process and reaches a saturation value at about 3 nm thickness. In the case of the

* Present address: Semikron GmbH, Nürnberg.
** Present address: BASF Ludwigshafen.

Reprint requests to Prof. Dr. P. Wißmann, Institut für Physikalische und Theoretische Chemie der Universität, Egerlandstraße 3, 8520 Erlangen.

0340-4811 / 86 / 0400-0665 $ 01.30/0. – Please order a reprint rather than making your own copy.

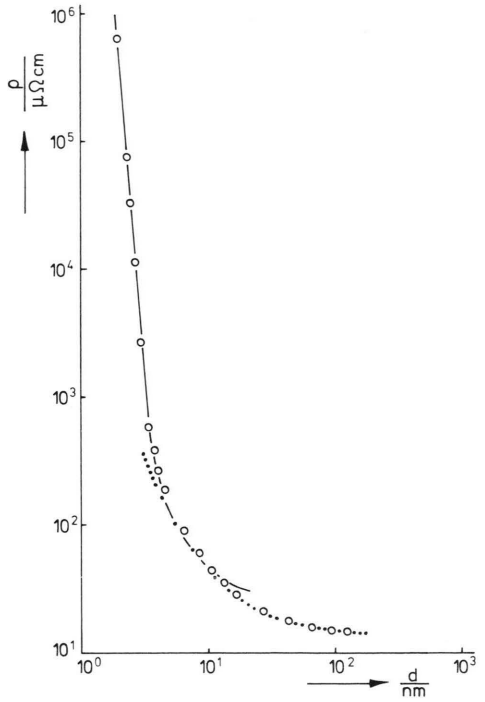

Fig. 1. Resistivity ϱ of ultra-thin Pd films deposited at room temperature on glass substrates, in dependence on mean film thickness d. (○) experimental values. (——) recalculated with the help of a statistical model [15]. (....) recalculated with the help of the scattering hypothesis (Equation (3)).

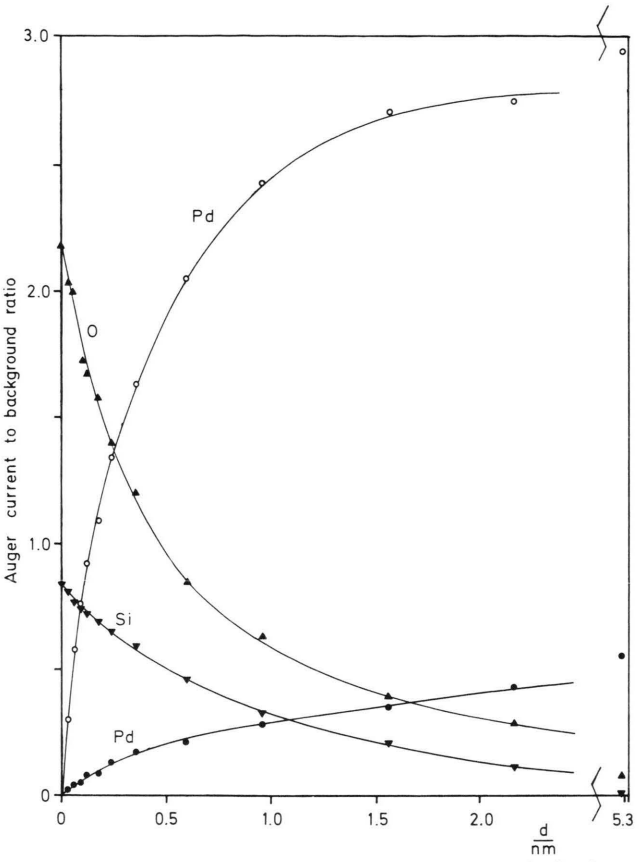

Fig. 2. Auger signal strengths vs. mean thickness d of Pd overgrowth on SiO_2. ○ Pd (330 eV), ● Pd (2485 eV), ▲ O (507 eV), ▼ Si (1606 eV).

2485 eV (●) peak no saturation is found up to 6 nm thickness, which is due to the higher escape depth of the high energy Auger electrons. Obviously laterial growth of the Pd film predominates. On the other hand, the decrease of the silicon 1606 eV peak (▼) and the oxygen 507 eV peak (▲) with increasing palladium thickness d is weaker than expected from the relation

$$I = I_0 \, e^{-d/\mu l_0}, \tag{2}$$

where l_0 is the escape depth ($l_0 \approx 1$ nm [11]). The characteristic constant μ depends on the geometry of the analyzer; for a cylindrical analyzer we obtain $\mu = 0,74$ [12]. Figure 2 indicates that, contrary to the prection of (2), substantial silicon and oxygen peak intensities are detected at relatively high palladium thicknesses. This result leads to the conclusion that portions of the substrate are not covered by Pd, i.e. the films have an island-like shape. A direct verification of this behaviour is provided by transmission electron microscopy (TEM).

4. TEM Measurements

In a separate apparatus we have deposited 50 nm thick SiO_2 layers on NaCl single-crystal substrates. After dissolving the NaCl in water and attaching the SiO_2 to net supports the palladium was evaporated as described above. The samples obtained in this manner were put in a transmission electron microscope (Philips EM 400). The mean thickness of the palladium films was determined after completion of all investigations by means of quantitative x-ray fluorescence analysis.

Four typical micrographs are shown in Figure 3. At a mean thickness of 0.4 nm one can easily detect the formation of small particles, which are clearly separated from each other. At a thickness of 1.6 nm, coalescence results in a polycrystalline structure of the islands as is obvious from the variation in the Bragg contrast within the aggregates in Figure 3 b.

The shape of these aggregates is rather irregular so that meander-like current paths are formed. From the relatively highly covered area at a rather small mass deposit we may conclude that the paths are only a few atom layers thick. The length is restricted to some hundreds of nm. At $d = 2.5$ nm conducting paths develop through the whole film. The mean width of the paths is roughly about 4 nm. At $d = 5.3$ nm a more coherent film structure develops. For thicknesses above 8 nm a continuous polycrystalline structure is formed where the mean crystallite extension in the film plane approaches to the film thickness.

The corresponding electron diffraction patterns of the Pd films are shown in Figure 4. It is clearly seen how the crystalline structure and a weak [111] fibre texture develops with increasing thickness. The angular positions of the peak maxima were evaluated on the basis of Bragg's equation, and a good agreement between the derived lattice parameter and literature data for bulk Pd was found.

5. X-Ray Diffraction Texture Analysis

In order to establish the texture properties some samples were removed from the UHV apparatus and put into the sample holder of a texture analyzer. For details of the experimental arrangement the reader is referred to Fischer et al. [13]. Usually the resulting intensities are plotted into a pole figure at a fixed glancing angle (θ_{111}). Since no dependence on the azimuth angle φ was observed, however, we restrict ourselves to plotting the reduced intensities $I \cos \beta$ [13] vs. the inclination angle β as shown in Fig. 5 for a 12 nm thick Pd film.

The half width of the main maximum is about 30° indicating that the film exhibits a substantial mosaic structure, i.e. the various crystallites are remarkably inclined against the film surface. At $\beta = 70.5°$ again the (111) planes should be positioned at a reflection angle but no destinct side maxima are detected due to the limited sensitivity of the texture analyzer used here. The half width decreases with increasing film thickness.

6. Discussion and Conclusions

From the results presented above it is concluded that the strong changes in resistivity for $d \leqq 8$ nm must be ascribed to a partial cracking of the film. Not the electron tunnelling between separated metal islands [14] but the formation of narrow current paths and meanders with small storing of palladium atoms are probably responsible for the steep increase of the resistivity.

For a more quantitative description the lengths and widths of the paths should be recorded in dependence on the deposited amount of palladium. This seems to be impossible at the time being. We therefore have restricted ourselves to the application of a simple statistical model for the simulation of the growth process. Details of the simulation have been described in a previous paper [15]. We divided the substrate into 10×10 small cells and bombarded it with clusters of a definite size with the help of a random generator. The resistivity was then calculated using normal network analysis. The result of the calculation is represented by the solid curve in Fig. 1 using the parameters $\alpha = 1000$ and $d_0 = 4$ nm. $\alpha = 1000$ implies that electron tunnelling does not play an important role in the present case [15]. The mean cluster size of $d_0 = 4$ nm seems to be a reasonable value because it can be roughly identified with the width of the current paths.

The very crude assumptions underlying the described model are obvious. Coagulation processes and a possible size distribution of the crystallites are excluded from the present consideration. Here further efforts are necessary to bring the model into better agreement with physical reality.

In addition to the theoretical curve based on the statistical model Fig. 1 contains a further curve (dotted curve) which describes the influence of grain boundary scattering and surface roughness on the resistivity according to [16]

$$\frac{\varrho}{\varrho_0} = 1 + \frac{C}{d} + \frac{CB^2}{d^3}, \tag{3}$$

where C is the scattering constant and B the mean roughness amplitude. The evaluation of the experimental data of Fig. 1 with the help of (3) leads to $\varrho_0 = 13\ \mu\Omega$ cm, $C = 15$ nm and $B = 7.5$ nm. Obviously this curve can satisfactorily explain the higher range of the thickness region investigated here. Around $d = 8$ nm there exists a thickness region where both models predict an identical resistivity behaviour of the palladium films.

Thanks are due to the Deutsche Forschungsgemeinschaft for generous financial support.

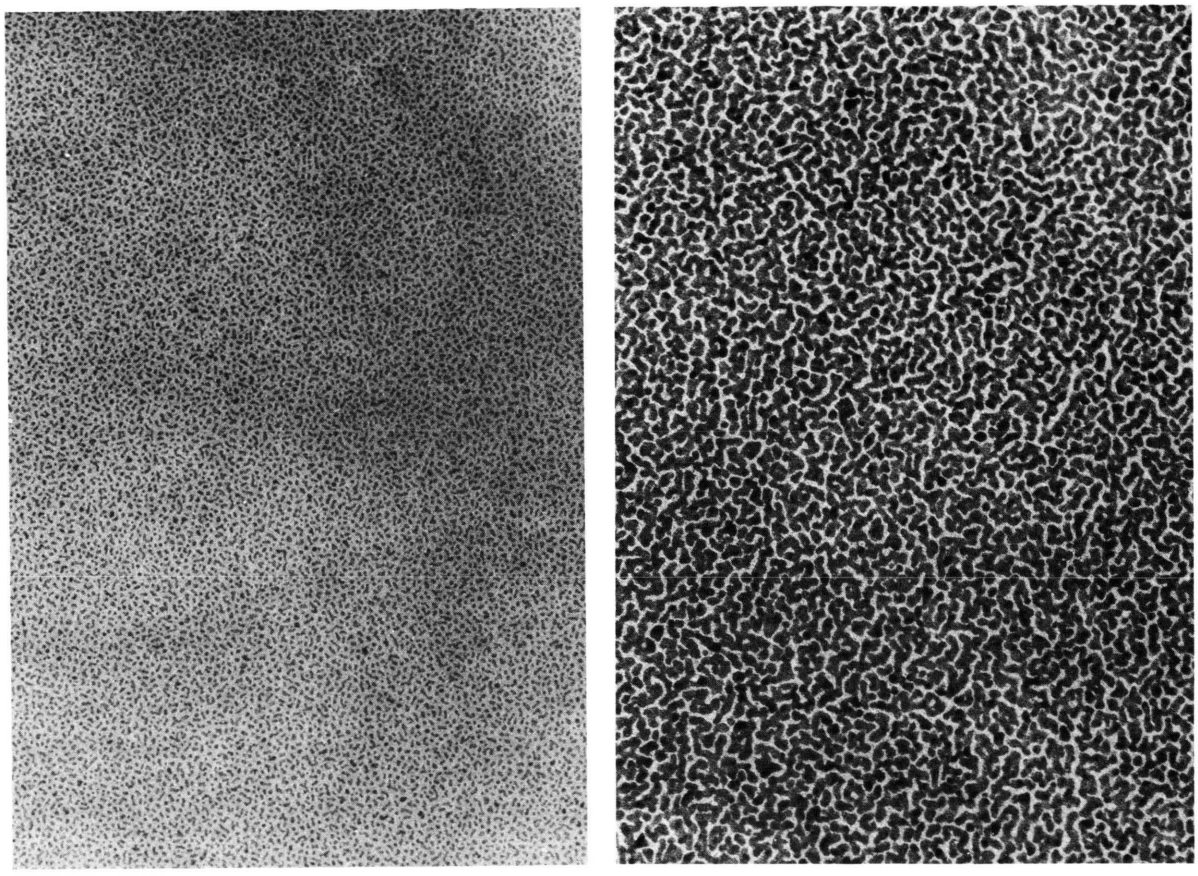

a) b)

Fig. 3.

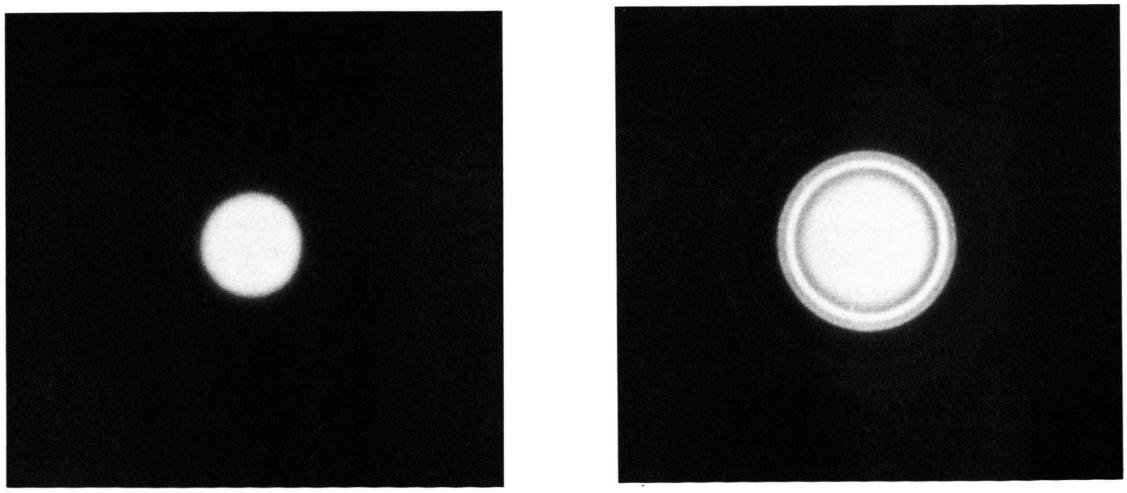

a) b)

Fig. 4.

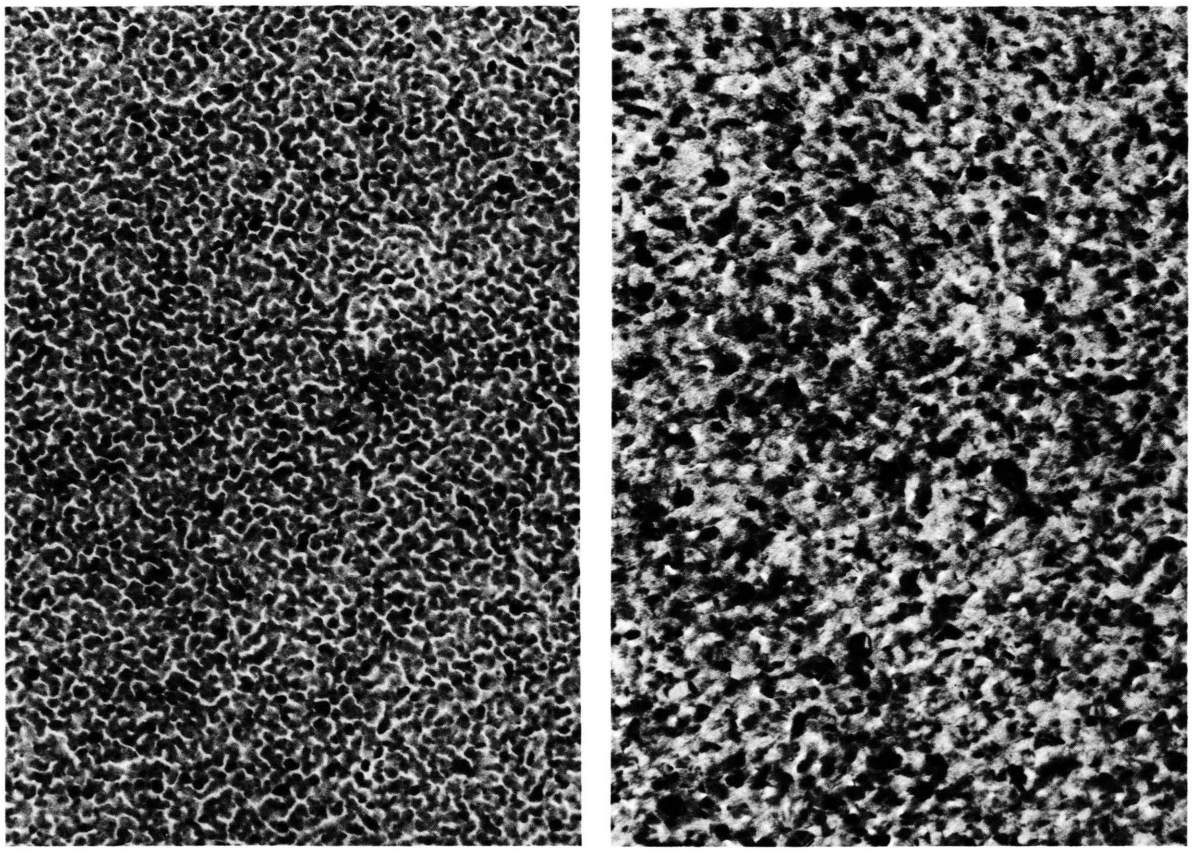

c) d)

Fig. 3. Electron micrographs of Pd deposited at room temperature on SiO_2. The mean thicknesses of Pd are a) 0.4; b) 1.6; c) 2.5 and d) 5.3 nm. The widths of the micrographs correspond to 250 nm.

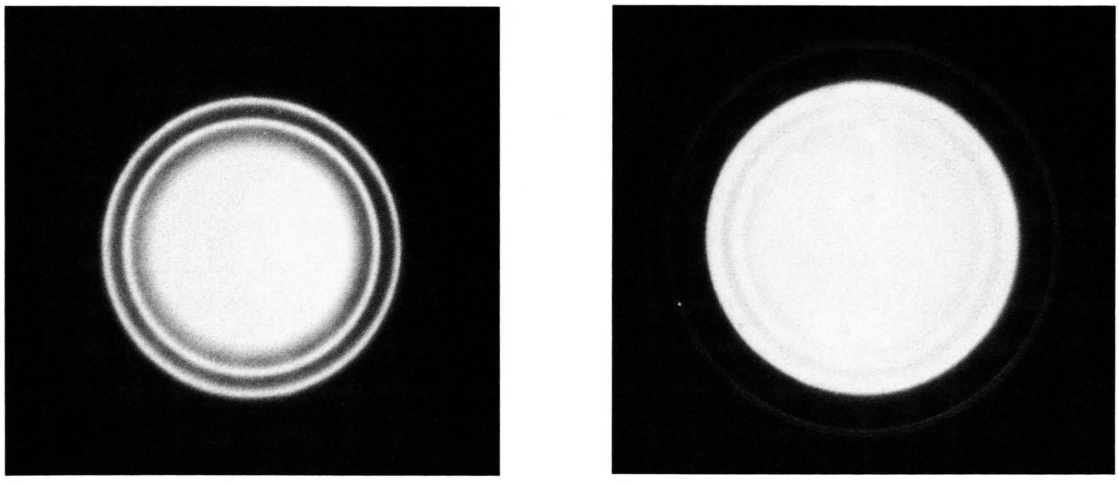

c) d)

Fig. 4. Electron diffraction patterns of the Pd films of Figure 3.

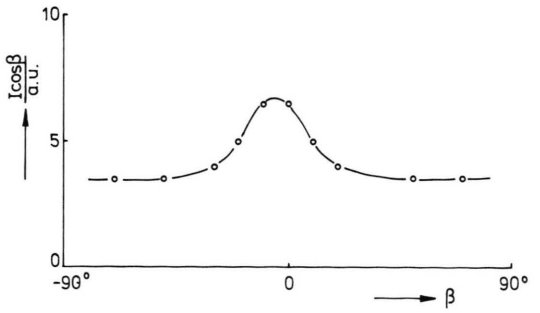

Fig. 5. Reduced intensity $I \cos \beta$ versus the inclination angle β (texture profile) for a 12 nm thick Pd film.

[1] C. Nylander, M. Armgarth, and C. Svensson, in: Insulating Films on Semiconductors (M. Schulz and G. Pensl, eds), Springer Series in Electrophysics **7,** 195 (1981).
[2] T. Engel and G. Ertl, in: The Chemical Physics of Solid Surfaces and Heterogeneous Catalysis Vol. 4 (D. A. King and D. P. Woodruff, eds), Elsevier, Amsterdam 1982, pp. 73.
[3] R. Suhrmann and G. Wedler, Z. angew. Physik **14,** 70 (1962).
[4] G. Wedler and G. Alshorashi, Thin Solid Films **74,** 1 (1980).
[5] R. Anton and H. Poppa, Proc. 10th Internat. Congr. Electron Microscopy, Hamburg 1982, Deutsche Ges. für Elektronenmikroskopie (Publ.), Frankfurt 1982, p. 509.
[6] J. F. Hamilton and P. C. Logel, Thin Solid Films **23,** 89 (1974).
[7] R. Anton and H. Poppa, Proc. 10th Internat. Congr. Electron Microscopy, Hamburg 1982, Deutsche Ges. für Elektronenmikroskopie (Publ.), Frankfurt 1982, p. 511.
[8] J. F. Hamilton, D. R. Preuss, and G. R. Apai, Surf. Sci. **106,** 146 (1981).
[9] D. Dayal, P. Rudolf, and P. Wißmann, Thin Solid Films **79,** 193 (1981).
[10] R. Anton, Thin Solid Films **120,** 293 (1984).
[11] C. R. Brundle, J. Vac. Sci. Technol. **11,** 212 (1974).
[12] M. P. Seah, Surf. Sci. **32,** 703 (1972).
[13] W. Fischer and P. Wißmann, Z. Naturforsch. **31a,** 190 (1976).
[14] C. A. Neugebauer and M. B. Webb, J. Appl. Phys. **33,** 74 (1962).
[15] H.-U. Finzel and P. Wißmann, Z. Naturforsch. **40a,** 161 (1985).
[16] H.-U. Finzel and P. Wißmann, Ann. Phys. **42** (1985).